# Edge Termination for III-Nitride Vertical Power Devices Using Polarization Engineering

Matthew R. Peart and Jonathan J. Wierer, Jr., *Senior Member, IEEE*

***Abstract*— A method for edge termination utilizing polarization-induced charge for GaN vertical power devices is presented. The polarization edge termination is simulated on a GaN power diode and consists of a 5-nm-thick n-type AlGaN layer on top of a p-type GaN layer that is located at the periphery of the main p-n junction. The spontaneous and piezoelectric polarization present in III-nitrides result in fixed charges at the AlGaN/GaN heterointerface, and the p-GaN layer becomes depleted at this interface under reverse bias. Numerical simulations show that this AlGaN/GaN heterointerface can be engineered to control the depletion region under reverse bias to prevent localization of electric fields and premature avalanche breakdown. Nearly parallel-plate reverse breakdown performance can be achieved. In addition, a simple analytical model based on charge balancing predicts the performance of this edge termination method.**

***Index Terms*— Aluminum gallium nitride (AlGaN), edge termination, field plate, gallium nitride (GaN), junction termination extension (JTE), polarization, power diode, power semiconductor devices, vertical devices.**

## I. Introduction

WIDE bandgap semiconductor power devices are being developed as alternatives to conventional Si power devices and for new applications. Advantages of wide bandgap semiconductors include higher operating voltages, higher power densities, and faster switching speeds. SiC and gallium nitride (GaN) power devices have progressed to become commercially viable competitors to Si for some applications [1], [2]. In particular, GaN diodes with avalanche breakdown voltages up to 5 kV with resultant electric field strengths around 3.5 MV/cm have been achieved [3]–[7].

In order to realize maximum breakdown voltages, localization of the electric field must be prevented. This field localization results from crowding of the depletion layer under the reverse bias that is due to the finite size of the device, and it occurs at contact discontinuities or device edges. Creating edge termination structures can be difficult in GaN. For example, it is difficult to selectively create the doped layers although there has been some recent progress [8], [9]. The most successful edge terminations are formed by implantation-based methods to create junction termination extensions (JTEs), field rings, bilayer structures, and bevels [4]–[6], [10]–[12].

The III-nitrides have high piezoelectric and spontaneous polarization, and heterointerfaces can have large amounts of polarization fixed charge. This property is most successfully used in aluminum GaN (AlGaN) high electron mobility transistors to create highly conductive channels [13]. It is also possible that this polarization-induced charge could be used for edge termination similar to a field plate wherein the additional charge is used to expand the depletion region under high reverse bias [14]. By properly engineering the heterointerfaces, one can control the polarization sheet charge.

In this article, the design of an edge termination using the polarization-induced sheet charge is demonstrated for III-nitride power devices. An AlGaN layer is placed on the p-GaN layer at the periphery of the main p-n junction, and this creates a positive charge and depletion of the p-GaN layer at the heterointerface that spreads the electric field under reverse bias. This charge can be tuned with Al composition, thickness, and dopant concentration within the AlGaN layer. Numerical simulations show nearly parallel-plate reverse bias performance. In addition, a simple analytical model is presented, which can predict the simulation results.

## II. Design and Simulation

A 2-D cross-sectional schematic of the simulated device is shown in Fig. 1. The vertical p-n power junction consists of a 200-nm-thick $p^+$-type layer, a 10-$\mu$m-thick n-type drift layer with a Si concentration [Si] of $2 \times 10^{16}/cm^3$, and a 2-$\mu$m-thick $n^+$-type contact layer with a [Si] of $10^{19}/cm^3$ on the bottom. Ohmic contacts are placed on either side with the top 20-$\mu$m-wide p-contact, only contacting the left-hand side. A nearly intrinsic i-GaN layer is added with a donor density of $10^{15}/cm^3$ (lower donor concentrations work too), which simulates a deadening implant and creates a simple boundary condition at the edge of the device. The edge of the device could have been equivalently simulated as a mesa terminated with a dielectric.

The edge termination consists of a 5-nm-thick $Al_xGa_{x-1}N$ layer that is 70-$\mu$m-wide on top of the $p^+$-GaN layer between the p-contact and the device edge. The $Al_xGa_{x-1}N$ edge termination layer is doped n-type with [Si] at $10^{17}/cm^3$.

Manuscript received October 7, 2019; revised December 4, 2019; accepted December 5, 2019. Date of publication January 8, 2020; date of current version January 27, 2020. This work was supported in part by the U.S. National Science Foundation under Award #1935295. The review of this article was arranged by Editor K. J. Chen. *(Corresponding author: Matthew R. Peart.)*

The authors are with the Department of Electrical and Computer Engineering, Lehigh University, Bethlehem, PA 18015 USA, and also with the Center for Photonics and Nanoelectronics, Lehigh University, Bethlehem, PA 18015 USA (e-mail: mrp211@lehigh.edu; jwierer@lehigh.edu).

Color versions of one or more of the figures in this article are available online at http://ieeexplore.ieee.org.

Digital Object Identifier 10.1109/TED.2019.2958485

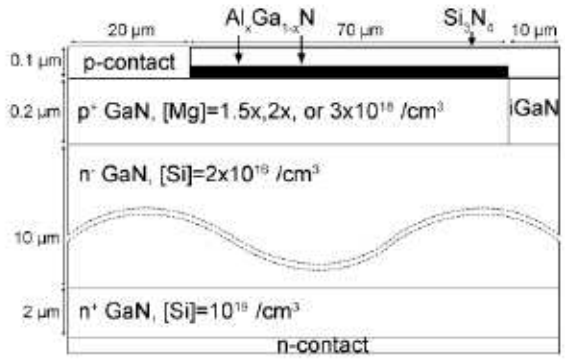


Fig. 1. Schematic cross section of the simulated GaN vertical p-n junction power diode. A highly doped $p^+$-GaN layer and lightly doped $n^-$-GaN drift form the main junction. A highly doped $n^+$ contact layer is at the bottom. A nearly intrinsic i-GaN layer is located in the right-hand side to isolate the edge of the device. The $Al_xGa_{x-1}N$ edge termination layer is the heavy black line at the top of the device between the p-contact and device edge.

In the simulation, $x$ is varied from 0 to 0.8, and the [Mg] is varied from $1.5 \times 10^{18}/\text{cm}^3$ to $3 \times 10^{18}/\text{cm}^3$ to change the polarization sheet charge or depletion width in the $p^+$-GaN layer. This p-type doping level is similar to GaN power diodes with record reverse breakdowns [3].

The device is simulated using Silvaco Atlas TCAD software building on previous reports [10], [11]. Best known values for spontaneous and piezoelectric polarization are taken from [15], and other relevant parameters are taken from [15] and [16]. The ionization coefficients were taken from experimental values from [17] and produce a critical electric field of 3.449 MV/cm for a $2 \times 10^{16}/\text{cm}^3$ doped drift layer. A reverse bias sweep, where the cathode is grounded and reverse bias is applied to the anode, is used to study the effect on the electric field and breakdown voltage $V_{br}$. Breakdown occurs when the reverse current reaches 100 $\mu$A. This threshold value for leakage was chosen as it was several orders of magnitude greater than the reverse leakage current.

## III. Results and Discussion

In this polarization edge termination method, the $Al_xGa_{1-x}N/p^+$-GaN interface has a positive charge. A 2-D electron gas (2DEG) forms in the $p^+$-GaN layer and partially screens this positive charge. However, under reverse bias, the 2DEG is fully depleted and, thus, allows the polarization charge to create a depletion region at the top of the $p^+$-GaN. This changes the conductivity in the $p^+$-GaN and spreads the electric field across the termination with the proper design. If designed properly, the diode should achieve the reverse breakdown performance of a parallel plate device. The parallel plate breakdown voltage $V_{br-pp}$ is calculated assuming a uniform doping distribution in the drift layer and an asymmetrically doped junction given by

$$V_{br-pp} = \frac{\epsilon_s E_c}{2qN_d} \quad (1)$$

where $E_c$ is the critical electric field, $N_d$ is the doping of the drift layer, $\epsilon_s$ is the permittivity, and $q$ is the fundamental charge. Using a critical electric field of 3.44 MV/cm results in a parallel-plate breakdown voltage of 1586 V.

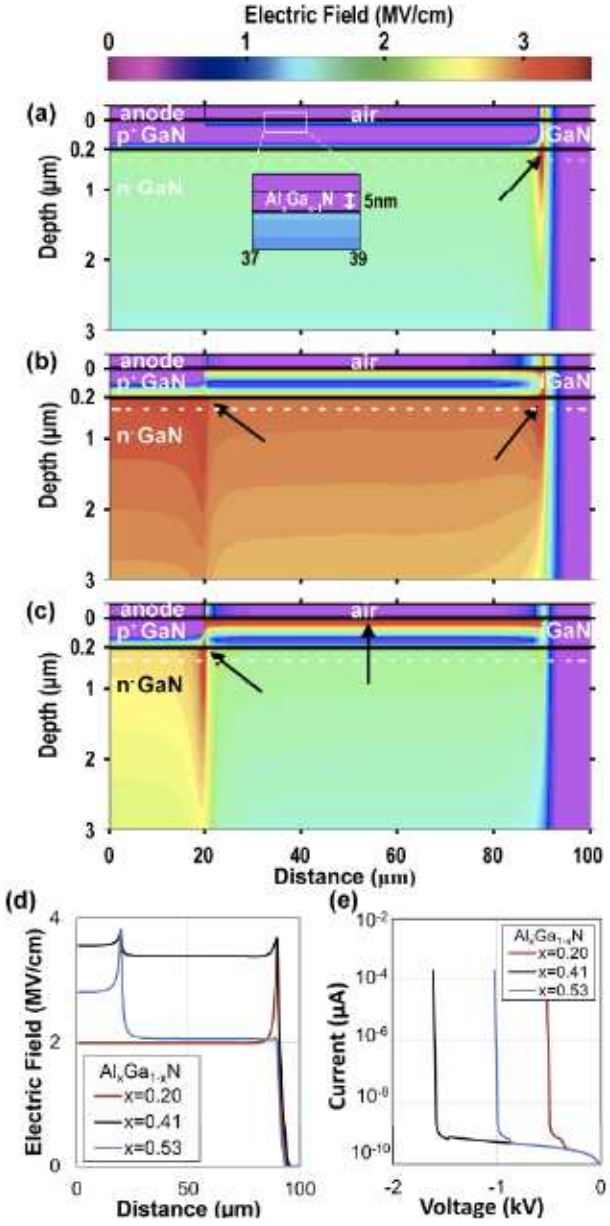


Fig. 2. 2-D electric field intensity plots of the power diode at breakdown with [Mg] = $2 \times 10^{18}/\text{cm}^3$ in the $p^+$-GaN layer and aluminum composition $x$ of (a) 0.2, (b) 0.41, and (c) 0.53. At $x = 0.2$, electric field is localized (arrow) at the edge of the device and results in $V_{br} = 520$ V. At $x = 0.41$, the electric field is spread optimally across the edge termination, resulting in the highest fields at the outside and p-contact edge (arrows) and results in a $V_{br} = 1616$ V. At $x = 0.53$, the electric field is localized at the p-contact and is also too high at the AlGaN/GaN heterointerface, lowering $V_{br} = 1020$ V. (d) 1-D electric field intensity near the junction at a position identified by the white dotted line in the 2-D plots. From the previous three cases, the flatness of the optimal 0.41 result demonstrates the optimized field spreading. (e) Reverse current versus voltage sweeps for the three different aluminum compositions.

Fig. 2 shows the 2-D plots of the electric field intensity with a different $x$ within the $Al_xGa_{x-1}N$ edge termination layer and with a [Mg] of $2 \times 10^{18}/\text{cm}^3$ in the $p^+$-GaN layer. At $x = 0.2$, there is insufficient polarization charge and not enough depletion at the top of the $p^+$-GaN to help spread

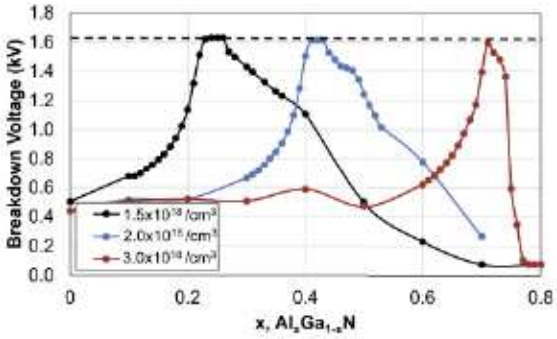


Fig. 3. Plot of the breakdown voltage versus Al composition, $x$, for [Mg] = $1.5 \times 10^{18}/cm^3$, $2 \times 10^{18}/cm^3$, and $3 \times 10^{18}/cm^3$ in the $p^+$-GaN layer. The horizontal dotted line is the parallel-plate breakdown voltage.

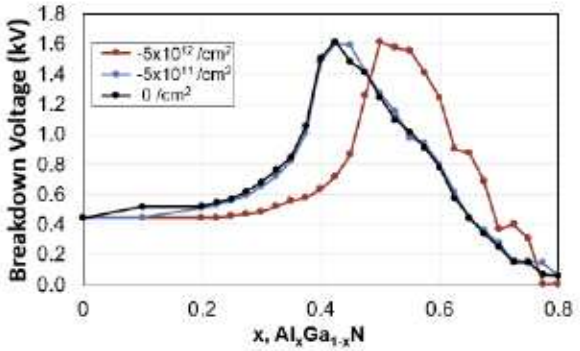


Fig. 4. Plot of the breakdown voltage versus Al composition, $x$, for [Mg] = $2 \times 10^{18}/cm^3$ and $Si_3N_4/Al_xGa_{1-x}N$ interface sheet charge densities of $0/cm^2$, $-5 \times 10^{11}/cm^2$, and $-5 \times 10^{12}/cm^2$.

the electric field, as shown in Fig. 2(a). The electric field is localized at the edge of the device (as it would be without edge termination) and $V_{br} = 520$ V. In Fig. 2(b), $x = 0.41$, and the $p^+$-GaN layer is depleted optimally by the polarization charge. The depletion width and electric field are spread uniformly across the edge termination length. For this $x$, $V_{br} = 1616$ V, and the diode has close to parallel-plate reverse breakdown performance. (Note that this $V_{br}$ is only limited by the drift layer thickness to control computation time and would be better with thicker drift layers.) As the aluminum composition is increased to $x = 0.53$ in Fig. 2(c), the polarization sheet charge further increases, and the edge of the depletion width is moved near the p-contact resulting in a large electric field and a lower $V_{br} = 1020$ V. Also, the sheet charge is too large, resulting in too much depletion and a large electric field across the top of the $p^+$-GaN layer. With further increases in $x$, the electric field increases at the AlGaN/GaN heterointerface and ultimately presents an upper limit on the polarization sheet charge possible for these simulations at $x \sim 0.78$. The horizontal electric fields near the junction are shown in Fig. 2(d), and the current versus voltage under reverse bias are shown in Fig. 2(e) for the three cases.

When the doping or thickness in the $p^+$-GaN layer is increased, the optimal $x$ will also increase to compensate for the increased charge required to expand the depletion width within the $p^+$-GaN layer. Conversely, as the doping in the $p^+$-GaN layer is reduced, the polarization charge required to balance the charge is reduced. This is demonstrated in Fig. 3 that shows the results of a series of simulations and plots of $V_{br}$ versus $x$ for [Mg] = $1.5 \times 10^{18}/cm^3$, $2 \times 10^{18}/cm^3$, and $3 \times 10^{18}/cm^3$ in the $p^+$-GaN. There is an optimal $x$ to properly balance the charge and achieve high $V_{br}$, and this optimum $x$ shifts with [Mg]. For the chosen layer's thicknesses, compositions, and doping, the optimum point shifts to higher $x$ as [Mg] is increased. The two lower [Mg] exhibit $V_{br}$ that gradually decreases with $x$ after peaking. At [Mg] = $3 \times 10^{18}/cm^3$, $V_{br}$ decreases more rapidly with $x$ after peaking due to the premature breakdown and large electric fields occurring at the top of the $p^+$-GaN layer for $x \sim 0.78$, as described earlier. No variations in $R_{on-sp}$ are observed in the simulations. The simulation for the forward voltage sweep results in a consistent value of $\sim 0.27$ m$\Omega \cdot cm^2$ that agrees closely with the theoretical value for the drift region resistance of $\sim 0.26$ m$\Omega \cdot cm^2$. The forward turn-on voltage is $\sim 3$ V. With a 10-$\mu$m drift layer thickness, the structure with the highest breakdown voltage has a figure of merit ($V_{br}^2/R_{on-sp}$) of $\sim 9.5$ GW/cm$^2$. It should also be noted that this edge termination also works for thicker and lower doped drift layers that operate in the higher breakdown voltages.

The simulations, thus far, do not include the potentially large negative-bound polarization charge at the air/$Al_xGa_{1-x}N$ interface and assumes that this interface is charge neutral. While this charge density can theoretically be as high as the polarization charge at the $Al_xGa_{1-x}N$/GaN interface, experimental values typically are in the range of $\sim 5.6 \times 10^{11}$–$1.3 \times 10^{12}/cm^2$ for passivated interfaces [18]. The remaining charge is compensated by electronic surface states. To gauge the impact of the uncompensated charge, the air at the surface is replaced with $Si_3N_4$, forming a $Si_3N_4/Al_xGa_{1-x}N$ interface, and additional simulations are performed for interface charge densities of $-1 \times 10^{11}/cm^2$ and $-5 \times 10^{12}/cm^2$. (Note higher interface charge densities do not converge in the simulation.) Fig. 4 shows the breakdown voltages versus composition for the different interface charges. For the simulation with interface charge densities of $-1 \times 10^{11}/cm^2$, the effect of the uncompensated charge is minimal. However, for charge densities of $-5 \times 10^{12}/cm^2$, which represents the upper bound of experimental measurements, the Al composition must be increased by 0.1 to reach the optimal breakdown voltage compared to the charge-neutral simulations. Proper knowledge of the $Si_3N_4/Al_xGa_{1-x}N$ charge will be necessary to experimentally realize this edge termination scheme. This surface charge could be controlled by using surface passivation techniques, as shown in GaN [18]–[21].

To understand the tradeoffs and guide the design, a simple predictive analytical model is constructed. This analytical model also helps in verifying the numerical simulations. Fig. 5(a) shows the band diagram at the breakdown of the top-most layers. The energy bands are bent over keV, and the p-GaN is in U shape. The p-GaN is bent down near the AlGaN layer due to the polarization interface charge at the AlGaN/p-GaN interface and bent down near the n-GaN drift layer because of the large reverse bias. There is a small portion in the

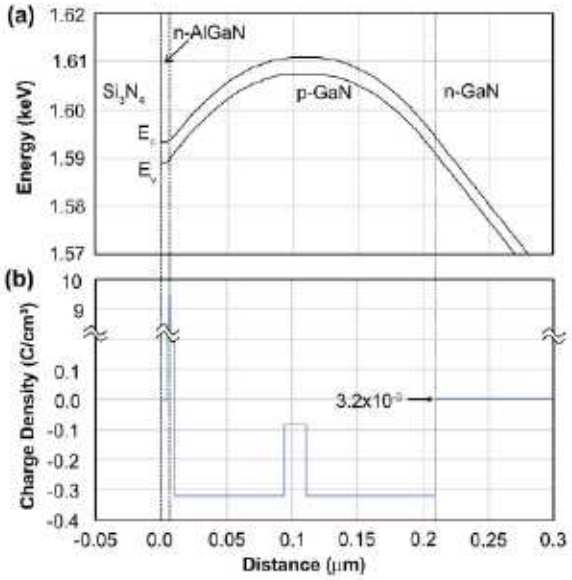


Fig. 5. Plot of (a) the energy bands (conduction $E_C$ and valence $E_V$), and (b) charge density of the top layers for the optimal case of $x = 0.41$ at breakdown. The reverse bias causes severe band bending with the p-GaN bent into a U shape caused by the fixed polarization interface charge at the AlGaN/p-GaN interface and reverse bias at the p-GaN/n-GaN interface. The band bending causes depleted charge in the p-GaN (negative) and n-GaN drift layer (positive). The smaller negative charge in the center of the p-GaN is caused by the flat band. The charge density of the n-GaN is small ($3.2 \times 10^{-3}$ C/cm$^3$) because of the large thickness of that layer.

middle of the p-GaN that is relatively flat. This band bending is manifested in the charge density given in Fig. 5(b). There are three regions of charge: the positive AlGaN/p-GaN interface charge, the negative charge in the p-GaN due to depleted acceptors, and the positive charge in the n-GaN drift layer due to depleted donors. The small variation in the middle of the p-GaN is due to the flat band and the U-shaped energy band.

The charge density plot helps in illustrating the total charge in the system to build a simple model. Assuming no free charge within the depletion regions under reverse bias (depletion approximation) and using Gauss's law, the sum of the sheet charge density $\rho_s$ required to balance the depleted charges in the n-GaN drift, p-GaN, and AlGaN layers outside the p-contact area can be expressed as

$$\rho_s = -q[N_{d,\text{drift}} X_{\text{drift}} - N_a W_p + N_{d,\text{ET}} W_{\text{ET}}] \tag{2}$$

where $N_{d,\text{drift}}$, $N_a$, and $N_{d,\text{ET}}$ are the doping in the n$^-$-GaN drift, p$^+$-GaN layer, and the AlGaN edge termination layer, respectively. $W_p$ and $W_{\text{ET}}$ are the depletion widths of the p$^+$-GaN and AlGaN edge termination layer, and $X_{\text{drift}}$ is the depletion width in the n$^-$-GaN drift layer all at the breakdown. The small rise in the middle of the p-GaN is ignored. In these simulations, $X_{\text{drift}}$ is equal to the total drift thickness. The drift layer thickness was chosen to be equal to the depletion width for this nonpunchthrough design.

In the numerical and analytical model, the polarization charge at the AlGaN/GaN heterointerface $P$ is given by [13]

$$P = -10^{-4}\left[0.0492x^2 + 0.0593x\right] \tag{3}$$

which includes the sum of the spontaneous and piezoelectric polarization charges. To achieve optimum breakdown voltage, the sheet charge density must equal to the polarization charge ($\rho_s = P$) and can be achieved by adjusting $x$ of the $Al_xGa_{1-x}N$. Using this condition and (1) and (2), the optimum $x$ for [Mg] $= 1.5 \times 10^{18}$/cm$^3$, $2 \times 10^{18}$/cm$^3$, and $3 \times 10^{18}$/cm$^3$ are $x = 0.23$, 0.41, and 0.69, respectively. These are close to the peak breakdown values found by numerical simulations, as shown in Fig. 3, and this verifies this simple model and the simulations.

Other variations beyond AlGaN/GaN structures are possible for polarization edge termination. For example, AlInN could be used as an alternative providing more control of the piezoelectric charge with the ability to change from tensile to compressive strain. If the termination structure is required to be on n-type layers, such as the case of a Schottky diode with an n-GaN drift layer, then an InGaN edge termination layer could be used. This would create a negative charge on the top of the drift layer and extend the depletion region more like a traditional JTE. Another embodiment is to segment the layer to create field rings [14]. Finally, polarization edge terminations may be used as an edge termination for not only power diodes but also for other III-nitride-based power devices.

This edge termination is different from other forms because it is formed during epitaxial growth instead of during device processing. The growth of AlGaN on GaN is well known, but there are some developments needed to realize this edge termination. If the structure is grown in one step, then additional fabrication steps are required to remove the AlGaN from the p-contact area and, successfully, form an ohmic contact. Conversely, AlGaN could be selectively grown in a second growth step. The simulations show that any gap between the p-contact and edge termination layer results in nominal differences in the breakdown voltage.

## IV. Conclusion

A method for edge termination utilizing polarization-induced charge is presented for GaN vertical power devices by numerical simulation. With the proper composition, thickness, and doping in the AlGaN edge termination and p-GaN layer, nearly parallel-plate reverse voltages can be achieved. A simple analytical model using charge balancing predicts the optimum edge termination layer conditions.

## References

[1] T. P. Chow, "High-voltage SiC and GaN power devices," in *Proc. Microelectron. Eng. SPEC ISS*, Sep. 200, vol. 83, no. 1, pp. 112–122, doi: 10.1109/BIPOL.2004.1365779.

[2] J. Y. Tsao *et al.*, "Ultrawide-bandgap semiconductors: Research opportunities and challenges," *Adv. Electron. Mater.*, vol. 4, no. 1, Dec. 2018, Art. no. 1600501, doi: 10.1002/aelm.201600501.

[3] H. Ohta *et al.*, "Vertical GaN p-n junction diodes with high breakdown voltages over 4 kV," *IEEE Electron Device Lett.*, vol. 36, no. 11, pp. 1180–1182, Nov. 2015, doi: 10.1109/LED.2015.2478907.

[4] T. Maeda *et al.*, "Parallel-plane breakdown fields of 2.8-3.5 MV/cm in GaN-on-GaN p-n junction diodes with double-side-depleted shallow bevel termination," in *IEDM Tech. Dig.*, San Francisco, CA USA, Dec. 2018, pp. 30.1.1–30.1.4, doi: 10.1109/IEDM.2018.8614669.

[5] H. Ohta, K. Hayashi, F. Horikiri, M. Yoshino, T. Nakamura, and T. Mishima, "5.0 kV breakdown-voltage vertical GaN p–n junction diodes," *Jpn. J. Appl. Phys.*, vol. 57, pp. 04FG09-1–04FG09-4, Feb. 2018, doi: 10.7567/JJAP.57.04FG09.

[6] I. C. Kizilyalli, T. Prunty, and O. Aktas, "4-kV and 2.8-m$\Omega$-cm$^2$ vertical GaN p-n diodes with low leakage currents," *IEEE Electron Device Lett.*, vol. 36, no. 10, pp. 1073–1075, Oct. 2015, doi: 10.1109/LED.2015.2474817.

[7] A. M. Armstrong *et al.*, "High voltage and high current density vertical GaN power diodes," *Electron. Lett.*, vol. 52, no. 13, pp. 1170–1171, Jun. 2016, doi: 10.1049/el.2016.1156.

[8] Y. Zhang *et al.*, "Vertical GaN junction barrier Schottky rectifiers by selective ion implantation," *IEEE Electron Device Lett.*, vol. 38, no. 8, pp. 1097–1100, Aug. 2017, doi: 10.1109/LED.2017.2720689.

[9] J. Hu, Y. Zhang, M. Sun, D. Piedra, N. Chowdhury, and T. Palacios, "Materials and processing issues in vertical GaN power electronics," *Mater. Sci. Semicond. Process.*, vol. 78, pp. 75–84, May 2018, doi: 10.1016/j.mssp.2017.09.033.

[10] J. J. Wierer, J. R. Dickerson, A. A. Allerman, A. M. Armstrong, M. H. Crawford, and R. J. Kaplar, "Simulations of junction termination extensions in vertical GaN power diodes," *IEEE Trans. Electron Devices*, vol. 64, no. 5, pp. 2291–2297, May 2017, doi: 10.1109/TED.2017.2684093.

[11] J. R. Dickerson *et al.*, "Vertical GaN power diodes with a bilayer edge termination," *IEEE Trans. Electron Devices*, vol. 63, no. 1, pp. 419–425, Jan. 2016, doi: 10.1109/TED.2015.2502186.

[12] I. C. Kizilyalli, A. P. Edwards, H. Nie, D. Disney, and D. Bour, "High voltage vertical GaN p-n diodes with avalanche capability," *IEEE Trans. Electron Devices*, vol. 60, no. 10, pp. 3067–3070, Oct. 2013, doi: 10.1109/TED.2013.2266664.

[13] U. K. Mishra, P. Parikh, and Y.-F. Wu, "AlGaN/GaN HEMTs-an overview of device operation and applications," *Proc. IEEE*, vol. 90, no. 6, pp. 1022–1031, Nov. 2002, doi: 10.1109/JPROC.2002.1021567.

[14] B. J. Baliga, *Fundamentals of Power Semiconductor Devices*. New York, NY, USA: Springer, 2008.

[15] S. L. Chuang, *Physics of Photonic Devices*, 2nd ed. Hoboken, NJ, USA: Wiley, 2009.

[16] J. Piprek, *Nitride Semiconductor Devices: Principles and Simulation*. Weinheim, Germany: Wiley, 2007.

[17] B. J. Baliga, "Gallium nitride devices for power electronic applications," *Semicond. Sci. Technol.*, vol. 28, Jun. 2013, Art. no. 074011, doi: 10.1088/0268-1242/28/7/074011.

[18] B. S. Eller, J. Yang, and R. J. Nemanich, "Electronic surface and dielectric interface states on GaN and AlGaN," *J. Vac. Sci. Technol. A, Vac. Surf. Films*, vol. 31, no. 5, 2013, Art. no. 050807, doi: 10.1116/1.4807904.

[19] T. Hashizume, S. Ootomo, S. Oyama, M. Konishi, and H. Hasegawa, "Chemistry and electrical properties of surfaces of GaN and GaN/AlGaN heterostructures," *J. Vac. Sci. Technol. B, Microelectron.*, vol. 19, pp. 1675–1681, Aug. 2001, doi: 10.1116/1.1383078.

[20] R. Yeluri, B. L. Swenson, and U. K. Mishra, "Interface states at the SiN/AlGaN interface on GaN heterojunctions for Ga and N-polar material," *J. Appl. Phys.*, vol. 111, pp. 043718-1–043718-5, Feb. 2012, doi: 10.1063/1.3687355.

[21] M. Capriotti *et al.*, "Fixed interface charges between AlGaN barrier and gate stack composed of *in situ* grown SiN and $Al_2O_3$ in AlGaN/GaN high electron mobility transistors with normally off capability," *Appl. Phys. Lett.*, vol. 104, pp. 113502-1–113502-5, Mar. 2014, doi: 10.1063/1.4868531.